2018 European Control Conference (ECC)
June 12-15, 2018. Limassol, Cyprus

Optimal Control of Solar Thermal Plants with Energy Storage*

Sergio J. Navas[1], Francisco R. Rubio[2], Pedro Ollero[3] and João M. Lemos[4]

Abstract— **This paper describes and assesses an optimal strategy to control distributed solar collector fields with thermal storage systems, especially during days with partial radiation due to the passage of clouds. The main objective of these control strategies is to maximize the thermal energy stored during different situations in which different parts of the solar field receive different degrees of solar radiation while keeping the net electrical power produced close to its set point. Simulations were carried out using three connected models, one for the solar field (taking into account all of its loops individually), that includes the passage of clouds, another one for the thermal storage system, and finally one for the power cycle. The solar field simulated is a small demonstration plant, in which it is assumed that all the loops have the same characteristics; and the nominal power range of the Rankine cycle is 800-2330kW.**

I. INTRODUCTION

For some time now, there has been a growing interest in the use of solar energy, and specifically of solar thermal power plants. The Solar Thermal Power Plants (CSP) are systems used to get electric power from solar energy by pre-transforming it into thermal energy. This paper focuses on parabolic trough solar fields, that consist of a collector field (figure 1), a power cycle, a thermal storage system, and auxiliary elements such as pumps, pipes, and valves (figure 2). The solar collector field collects solar radiation and focuses it onto a tube in which a heat transfer fluid, such as thermal oil, circulates. The oil is heated up and then used by the power cycle to produce high pressure steam in a boiler, and electricity by expanding it in a turbo-generator.

The main goal of a parabolic trough solar field is to collect solar energy in order to produce as much electrical power as possible. Normally, most of the solar thermal power plants try to achieve this objective by keeping the outlet oil temperature of the field around the maximum allowable value, that in this case is 400°C, imposed to prevent oil degradation. However, some studies like [15], and [7] show that this way to operate the field does not produce the best results of electrical power generated. In [15] it was suggested that the optimum strategy is based on adapting the oil outlet temperature to the incident solar radiation, keeping constant the superheating temperature increment of the steam, whereas in [7] it was proposed to change the outlet temperature set point according to the value of the solar radiation. Therefore, in [15] the controlled variable is the superheating temperature, while in [7] it is the oil outlet temperature. In this paper the issue of controlling optimally a field with partial radiation and a thermal storage system is handled, and to do so an entire field model is used in order to take into account not only the total incident radiation, but as well its distribution among each of the loops that constitute the solar field. With this model it is possible to simulate each loop of the field, instead of simulating only one of them and supposing that the behavior of the entire field is the same. In addition the thermal storage system is considered.

The use of a solar field model that individually takes into account all its loops was proposed in [1], but it was used to test a control strategy based on maximizing the outlet oil temperature of the field (until a maximum value of 400°C), which as said before it is not the optimal way to produce the maximum electrical power. However, in this paper this type of field model is used to assess a control strategy whose main objective is to maximize the thermal energy stored by maximizing the electrical energy that can be achieved with the mass flow and temperature sent to the storage system, while keeping constant an electrical power reference, especially during days with partial covering.

The paper is organized as follows: Section II describes the models of the solar field, passing clouds, power cycle, and storage system used for simulation purposes. Section III describes the control strategy assessed. Section IV shows the results obtained by simulations. Finally, the paper draws to a close with some concluding remarks.

Fig. 1. ACUREX distributed solar collector field

II. SYSTEM MODELING

The model of each of the parts that have been used to simulate the operation of a solar plant during days with

*This work was supported by the projects DPI2013-44135-R and DPI2015-70973-R granted by the Spanish Ministry of Science and Innovation.

[1]Sergio J. Navas is with the Department of Systems and Automatic Engineering, University of Seville, Spain snavas1@us.es

[2]Francisco R. Rubio is with the Department of Systems and Automatic Engineering, University of Seville, Spain rubio@us.es

[3]Pedro Ollero is with the Department of Chemical and Environmental Engineering, University of Seville, Spain ollero@us.es

[4]João M. Lemos is with INESC-ID, Instituto Superior Técnico, University of Lisbon, Portugal jlml@inesc-id.pt

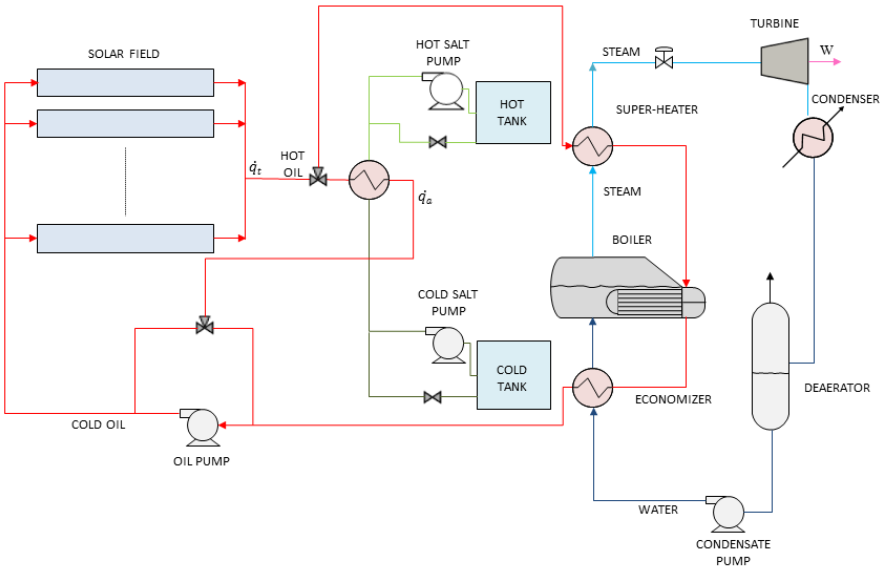

Fig. 2. Diagram of the solar field connected with the power cycle

partial covering is presented hereafter. These parts are: the solar collector field, the passage of the clouds, the power cycle, and the thermal storage system.

A. Solar Collector Field Model

The model of solar collector field is based on the model proposed by [3],[6],[8],[18], and [20]. Basically, this model can be used to simulate parabolic trough solar fields by selecting parameters like the number of active (the parts where the solar radiation reaches the tube) and passive (joints and other parts not reached by concentrated solar radiation) zones, the length of each zone, or the collector aperture. The solar field simulated in this paper is modeled using solar radiation data that correspond to the site of the Escuela Técnica Superior de Ingeniería de Sevilla. It is composed of 24 loops and has dimensions of 144x240 m. Each loop is modeled by the following system of partial differential equations that describe the energy balance:

Active zones

$$\rho_m C_m A_m \frac{\partial T_m}{\partial t} = In_0 G - H_l G(T_m - T_a) - dH_t(T_m - T_f), \quad (1)$$

Fluid element

$$\rho_f C_f A_f \frac{\partial T_f}{\partial t} + \rho_f C_f \dot{q}_t \frac{\partial T_f}{\partial x} = dH_t(T_m - T_f), \quad (2)$$

Passive zones

$$\rho_m C_m A_m \frac{\partial T_m}{\partial t} = -GH_p(T_m - T_a) - dH_t(T_m - T_f), \quad (3)$$

where the sub-index m refers to metal and f refers to the fluid. The model parameters and their units are shown in table I, and a more detailed description including their values can be found in [3]-[6]-[8]-[18]-[20].

TABLE I
SOLAR FIELD MODEL PARAMETERS AND VARIABLES DESCRIPTION

Symbol	Description	Units
t	Time	s
x	Space measured along the tube	m
ρ	Density	Kg/m^3
C	Specific heat capacity	J/(K kg)
A	Cross sectional area	m^2
T	Temperature	°C
$\dot{q}_t$	Oil flow rate	m^3/s
I	Solar radiation	W/m^2
n_0	Optical efficiency	Unit-less
G	Collector aperture	m
T_a	Ambient Temperature	°C
H_l	Global coefficient of thermal losses for active zones	W/(m^2 °C)
H_t	Coefficient of heat transmission metal-fluid	W/(m^2 °C)
H_p	Global coefficient of thermal losses for passive zones	W/(m^2 °C)
d	Pipe diameter	m

This solar field model is connected to a power cycle model and a storage system model (figure 2) as commented in section 1 and further described below. All models have to be simulated simultaneously because some of their variables are shared. Specifically, to simulate the field, the value of the inlet oil temperature is needed and it can only be obtained after solving the equations of the cycle model and the storage system model. At the same time, to simulate the power cycle and the storage system, the outlet temperature and the oil flow are needed. Therefore, the simulation of both models is an iterative process.

B. Modeling of the Passing Clouds

The modeling of the passing clouds is necessary to know how the solar radiation is distributed throughout the field. This can be achieved by creating a matrix that represents the whole field extension. Each element of the matrix is assigned the value of the incident solar radiation on that section at each time. The solar field has dimensions of 144x240 m so, if the field is divided in elements of 3x3 m, a 48x80 matrix is needed. The matrix is then put over the field in such a way that each element contains a fraction of an active or passive element. Figure 3 shows the fraction of the whole matrix that covers one loop of a generic field.

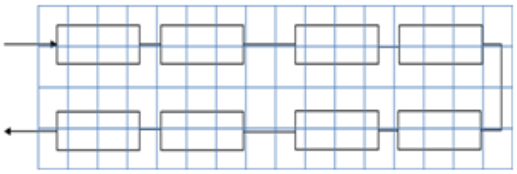

Fig. 3. Example of a fraction of the matrix over one loop of the field

The value of the radiation in each element of the matrix depends on the following parameters:

- The Direct Normal Irradiation (DNI) on the field.
- The direction of the route followed by the passing cloud (the angle formed by this direction and the direction followed by the thermal fluid, being 0 degrees the direction which is the same one followed by the thermal fluid and 90 degrees the perpendicular).
- The velocity of the passing cloud (determined by the number of elements of the matrix supposed to be traveled by the cloud every 39 seconds, which is the sample time of the field).
- The size of the cloud (a rectangular form is supposed, defined by the number of rows and columns that it covers).
- The attenuation factor, that is the value that multiplies the radiation in the zones where the cloud is present. This value varies between 0 and 1 depending on the radiation that the cloud allows to reach the field, being 0 the case in which no radiation reaches the field, and 1 the case in which all the radiation reaches it.

Once these values are set, the program calculates for each collector the mean value of radiation of every element of the matrix related with it. This mean value is assigned to the variable I of (1).

The velocity values used in the model are quite small. The reason of these values is that the solar field used for simulation is also small; therefore if real cloud velocities are simulated they scarcely produce any effect on the field due to the minimum residence time over the field. For that reason, in order to simulate a time of permanence similar to that of the commercial plants, a lower velocity is assumed. The effect of the other parameters was studied in [18].

C. Power Cycle Model

The Rankine power cycle simulated in this paper consists of an economizer, a boiler and a super-heater followed by a steam turbine. Following the path traveled by the oil flow (figure 2), it first enters into the super-heater where the steam flow is overheated to a certain temperature. After the super-heater, the oil flow is used to boil the water flow to produce saturated steam in the boiler. This process is carried out at a floating pressure to maximize the amount of heat exchanged. Finally, the oil flow is introduced into an economizer where it is used to preheat the boiler water, and is then recycled to the field. The steam generated in the super-heater flows into a high pressure turbine. This turbine has been modeled using the Willan's Line Method described in [24].

The complete and detailed model [20] was simulated using the software Engineering Equation Solver© and then with these simulation results two polynomial functions of the oil outlet temperature and mass flow were fitted to them to calculate the electrical power generated

$$W = 8230 - 49.96m_{oil} - 2.7m_{oil}^2 - 47.15T_{out} + 0.068T_{out}^2 + 0.54m_{oil}T_{out}, \quad (4)$$

and the oil temperature returning to the field

$$T_{in} = 340 + 1.78m_{oil} - 0.155m_{oil}^2 - T_{out} + 0.0011T_{out}^2 + 0.022m_{oil}T_{out}. \quad (5)$$

This simplification was necessary to reduce the simulation time, while keeping the error around 1%. In addition, the dynamic of the cycle was assumed to be like a first order model with a time constant of 100 seconds, that is the dynamic of the slowest part of the cycle, the boiler. The power cycle was modeled using the software Aspen Hysys© and the time constant was obtained by simulation.

The net electrical power produced by the field is the result of subtracting the power consumed by the oil pump to the power generated by the turbine. The power consumed by the pump and therefore the net electrical power can be obtained following the method used in [20].

D. Storage System Model

The storage system consists of a heat exchanger and two tanks of molten salts, whose composition is 40% of $NaNO_3$ and 60% of KNO_3. One of the tanks contains salt at 291°C, that is the salt that will be heated in the heat exchanger using the outlet oil of the solar field, whose thermal energy is intended to be stored. The salt flow, after having been heated in the heat exchanger, is sent to the other tank, where it is stored until it is needed to heat the oil of the solar plant in order to keep the electrical power production when there is no enough solar radiation. The storage system scheme can be seen in figure 2.

Each tank is modeled by a mass balance

$$\rho_s \frac{\partial V}{\partial t} = \dot{m}_{in} - \dot{m}_{out}, \quad (6)$$

and an energy balance

$$\rho_s C_s V \frac{\partial T}{\partial t} = C_s \dot{m}_{in}(T_{in} - T)$$
$$-C_s \dot{m}_{out}(T_{out} - T) - H_s(T - T_{amb}), \quad (7)$$

where V is the tank volume, $\dot{m}$ is the mass flow, T is the molten salt temperature in the tank, T_{amb} is the ambient temperature, H_s is the coefficient of thermal losses, ρ_s is the density and can be computed by

$$\rho_s = 2090 - 0.636T, \quad (8)$$

and C_s is the specific heat capacity defined by

$$C_s = 1443 - 0.172T. \quad (9)$$

The coefficient of thermal losses H_s has a value of 0.015 W/°C. This value has been calculated by assuming that the tank at maximum volume capacity, an ambient temperature of 25°C, and a salt temperature of 380°C loses 1°C of temperature per day.

The heat exchanger has been modeled by the equations

$$\begin{aligned} m_o C_{Po} T_{io} - Q_{St} &= m_o C_{Po} T_{oo}, \\ \dot{m} C_s T_{ist} + Q_{St} &= \dot{m} C_s T_{ost}, \\ Q_{St} &= U_{St} A_{St} LMTD_{St}, \end{aligned} \quad (10)$$

that form a system of three equations and three unknowns. The unknowns are the outlet oil and outlet salt temperatures, T_{oo} and T_{ost} respectively, and the heat exchanged Q_{St}. The value of the product of the thermal transmittance U_{St} and the exchange area A_{St} has been obtained by following the method explained in [20]. This value is 161.32 kJ/s °C. The rest of the variables are: the inlet oil and inlet salt temperatures, T_{io} and T_{ist} respectively; the oil and salt mass flows, m_o and $\dot{m}$ respectively; the oil specific heat capacity C_{Po}; and the logarithmic mean temperature difference $LMTD_{St}$ [20].

III. CONTROL STRATEGY

The control strategy presented in this paper consist of MPC controller that uses models of the field, the power cycle, and predictions of the passing clouds through the field, so that the controller calculates the optimum value of oil flow through the solar field $\dot{q}_t$ and oil flow sent to the storage system $\dot{q}_a$ that maximizes the thermal energy stored and maintain the electrical power at its set point. The solar collector field model used by the MPC is a simplification of the one used to simulated the real field (1)-(2), which assumes that the pipe is only divided in 6 parts of 80 meters instead of the divisions of 1 meter for passive zones and 3 meters for the active zones. The prediction of the passing clouds has been made assuming that the exact position of the cloud is known for each sampling interval of the prediction horizon, although the value of the incident solar radiation is supposed to be constant for each sampling interval, which adds some degree of error between the predicted value and the real one. The control structure can be seen in figure 4.

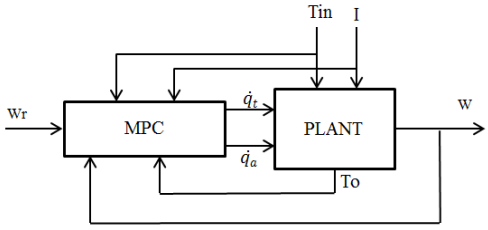

Fig. 4. MPC controller

The thermal energy stored and the error between the power reference and the controlled variable are considered along an extended period of time, from time $(k+1)h$ up to some horizon $(k+H)h$, where k denotes present discrete time, H is the prediction horizon, and h is the sampling interval, which in this case has a value of 39 seconds. Therefore, the aim is to select the values of $\dot{q}_t$ and $\dot{q}_a$ that maximizes the multistep cost function

$$J = \sum_{i=1}^{H} [-\lambda_1 (W_r - W_i)^2 - \lambda_2 (\Delta \dot{q}_t)^2 + (W_{max} - W_r)], \quad (11)$$

where W_r is the reference value, W_i is the net electrical power produced by the turbo-generator, and W_{max} is the maximum electrical power that would be produced if the total oil flow $\dot{q}_t$ were sent to the power cycle instead of sending the oil flow needed to produce W_i, that is $\dot{q}_t$-$\dot{q}_a$. Therefore, the maximization of J allows to achieve the maximum electrical power that would be produced by the plant, that in turns implies that the maximum thermal energy is stored (the difference between W_{max} and W_r is the value of the electrical energy that can be produced by the oil flow $\dot{q}_a$ sent to the storage system) while keeping the reference value of the electrical power produced (minimizing the quadratic error between W_r and W_i). In addition a term taking into account the variations in the variable $\dot{q}_t$ is included in order to avoid sudden changes. λ_1 and λ_2 are weighting sequences. The maximization of J is performed with a receding horizon strategy, using a prediction horizon of H=12 and a control horizon of 3.

The optimization is subject to restrictions in each loop oil outlet temperature ($T \leq 400$°C), oil flow ($0.133\ l/s \leq \dot{q}_t \leq 1.58\ l/s$), and the oil flow sent to the storage system ($0\ kg/s \leq \dot{q}_a \leq \dot{q}_t kg/s$). The optimization is carried out for each integration step by the function $fmincon$ in MATLAB. The optimum values of $\dot{q}_t$ and $\dot{q}_a$ are then sent as the new set points of the flow controllers, which manipulate the variable frequency drives. In this simulation, the dynamics of the flow controllers plus the dynamics of the pumps and the hydraulic circuit are assumed to be like a second order system.

IV. SIMULATION RESULTS

This section of the article shows the results obtained by simulations made with the models described in the previous

sections. The aim of these simulations is to assess the control strategy proposed in this paper, specially during days with partial radiation, that is, when different parts of the solar field receive different degrees of solar radiation. In this paper two cases has been studied, one with real solar radiation data measured by a sensor (in this case it is assumed that the solar radiation that reach each loop is the same and there is no prediction of the clouds), and another one with a simulated solar radiation with the passage of a certain type of clouds. The passing clouds for the second case have been simulated with the model described in section 2 with the following parameters: a matrix of 16x16, a velocity of 2 matrix elements per integration step, a direction of 45°, an attenuation factor of 0, and a time of passage of 15. This time of passage has been defined as the number of integration steps where there is no cloud over the field after the last one had abandoned it; that criteria means that during all the simulation there are passing clouds entering and leaving the field, separated by this time. The reference value of the electrical power W_{ref} is 1200 kW, and the values of λ_1 and λ_2 are 7 and 0.5 respectively. The solar radiation used for the first case can be seen in figure 5, and with that radiation curve the behavior of the controller can be seen in figures 6, 7, 8, and 9. It is clear that the controller can keep nearly constant the value of the electrical power produced, except when the value of the solar radiation is too low. The behavior of the total oil mass flow $\dot{q}_t$ and the storage oil mass flow $\dot{q}_a$ is right and without unacceptable changes. It can also be appreciated how the outlet oil temperature is changing according to the level of solar radiation, meaning that its optimum value it is not the maximum one (around 400°C).

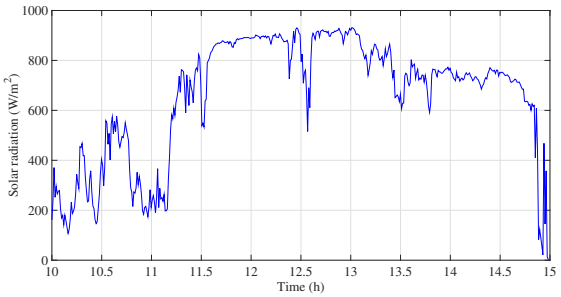

Fig. 5. Solar radiation measured

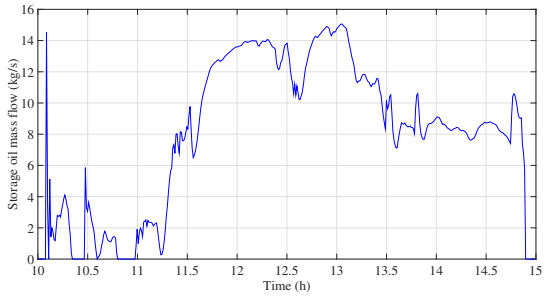

Fig. 6. Oil flow sent to the storage system

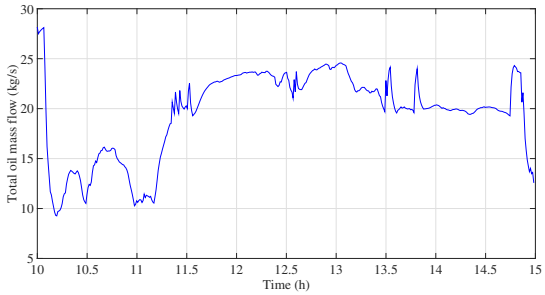

Fig. 7. Total oil flow of the field

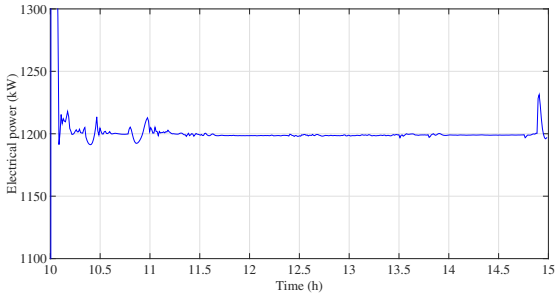

Fig. 8. Net electrical power

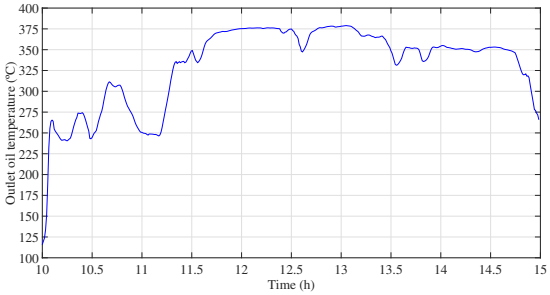

Fig. 9. Outlet oil temperature

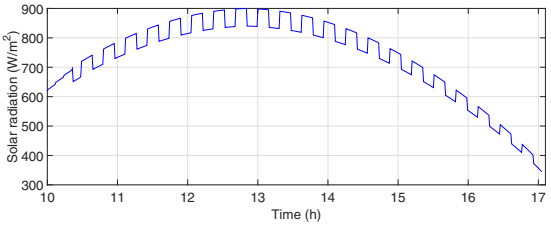

Fig. 10. Solar radiation simulated

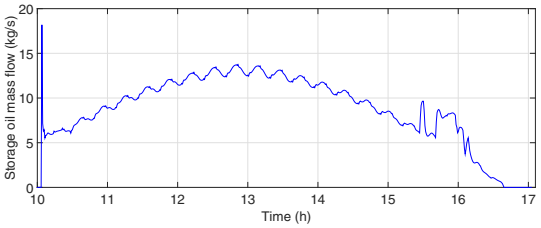

Fig. 11. Oil flow sent to the storage system

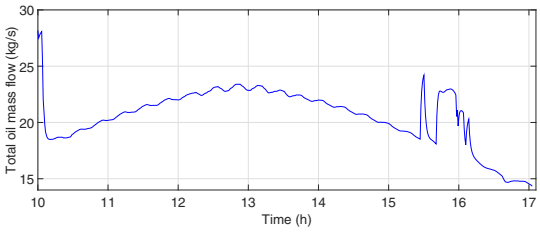

Fig. 12. Total oil flow of the field

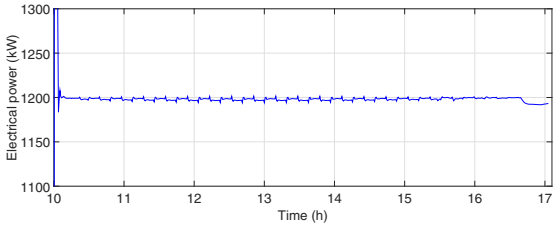

Fig. 13. Net electrical power

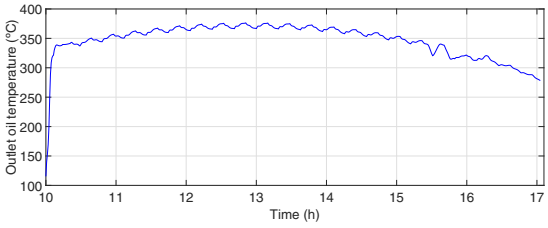

Fig. 14. Outlet oil temperature

In figure 10 the simulated solar radiation is presented. This radiation curves differ with the one shown in 5 mainly in the frequency of passage and the amount of solar radiation attenuated by the cloud. However, during this case the controller is also capable of keeping nearly constant the value of electrical power (figure 13). The behavior of $\dot{q}_t$ and $\dot{q}_a$ is also acceptable in this case, as can be seen in figures 12 and 11 respectively. In figure 14 it can be seen the optimum value of the outlet temperature as the solar radiation changes.

V. CONCLUSIONS

The main conclusion of this paper is that the MPC controller assessed can achieve the control objectives proposed (the maximization of the thermal energy stored and the achievement of the desired value of the net electrical power produced) during different situations in which different parts of the solar field receive different degrees of solar radiation.

REFERENCES

[1] ABUTAYEH, M., ALAZZAM, A. and EL-KHASAWNEH, B. (2014). *Balancing heat transfer fluid flow in solar fields.* Solar Energy, 105, 381-389.

[2] BARÃO, M., LEMOS, J. and SILVA, R. (2002). *Reduced complexity adaptive nonlinear control of a distributed collector solar field.* Journal of Process Control, 12-1, 131-141.

[3] CAMACHO, E. F., BERENGUEL, M. and RUBIO, F. (1997). *Advanced control of solar plants.* Springer-Verlag, London.

[4] CAMACHO, E. F., RUBIO, F. R., BERENGUEL, M. and VALENZUELA, L. (2007). *A survey on control schemes for distributed solar collector fields. Part I: Modeling and basic control approaches.* Solar Energy, 81-10, 1240-1251.

[5] CAMACHO, E. F., RUBIO, F. R., BERENGUEL, M. and VALENZUELA, L. (2007). *A survey on control schemes for distributed solar collector fields. Part II: Advanced control approaches.* Solar Energy, 81-10, 1252-1272.

[6] CAMACHO, E. F., BERENGUEL, M., RUBIO, F. R. and MARTÍNEZ, D. (2012). *Control of solar energy systems.* Springer-Verlag, London.

[7] CAMACHO, E. F. and GALLEGO, A. (2013). *Optimal operation in solar trough plants: A case study.* Solar Energy, 95, 106-117.

[8] CARMONA, R., (1985). *Análisis, modelado y control de un campo de colectores solares distribuidos con sistema de seguimiento en eje.* Ph.D. Thesis.

[9] CIRRE, C., BERENGUEL, M., VALENZUELA, L. and CAMACHO, E. F. (2007). *Feedback linearization control for a distributed solar collector field.* Control Engineering Practice, 15-12, 1533-1544.

[10] CIRRE, C., BERENGUEL, M., VALENZUELA, L. and KLEMPOUS, R. (2009). *Reference governor optimization and control of a distributed solar collector field.* European Journal of Operational Research, 193, 709-717.

[11] COLMENAR-SANTOS, A., MUNUERA-PEREZ, F., TAWFIK, M. and CASTRO-GIL, M. (2014). *A simple method for studying the effect of scattering of the performance parameters of parabolic trough collectors on the control of a solar field.* Solar Energy, 99, 215-230.

[12] GALLEGO, A. and CAMACHO, E. F. (2012). *Estimation of effective solar irradiation using an unscented kalman filter in a parabolic-trough field.* Solar Energy, 86-12, 3512-3518.

[13] GARCÍA, S. (2012). *Guía técnica de la energía solar termoeléctrica* Fenercom, Capítulo 1.

[14] LIMA, D., NORMEY-RICO, J. and SANTOS, T. (2016). *Temperature control in a solar collector field using filtered dynamic matrix control.* ISA Transactions, 62, 39-49.

[15] LIPPKE, F. (1995). *Simulation of the part-load behavior of a 30 MWe SEGS plant.* Report No. SAND95-1293, SNL, Albuquerque, NM, USA.

[16] MANZOLINI, G., GIOSTRI, A., SACCILOTTO, C., SILVA, P. and MACCHI, E. (2012). *A numerical model for off-design performance prediction of parabolic trough based solar power plants.* Journal of Solar Energy Engineering, Vol.134.

[17] MONTES, M., ABÁNADES, A., MARTÍNEZ-VAL, J. and VALDÉS, M. (2009). *Solar multiple optimization for a solar-only thermal power plant, using oil as heat transfer fluid in the parabolic trough collectors.* Solar Energy, 83-12, 2165-2176.

[18] NAVAS, S. J., RUBIO, F. R., OLLERO, P. and ORTEGA, M. G. (2016). *Modeling and simulation of parabolic trough solar fields with partial radiation.* XV European Control Conference, 31-36.

[19] NAVAS, S. J., RUBIO, F. R. and OLLERO, P. (2017). *Optimum control of parabolic trough solar fields with partial radiation.* IFAC-PapersOnLine, Vol.50-1, 109-114.

[20] NAVAS, S. J., OLLERO, P. and RUBIO, F. R. (2017). *Optimum operating temperature of parabolic trough solar fields.* Solar Energy, 158, 295-302.

[21] PRICE, H., LUPFERT, E., KEARNEY, D., ZARZA, E., COHEN, G., GEE, R. and MAHONEY, R. (2002). *Advances in parabolic trough solar power technology.* Solar Energy, 124-2, 109-125.

[22] RUBIO, F. R., CAMACHO, E. F. and BERENGUEL, M. (2014). *Control of solar collector fields.* Revista Iberoamericana de Automática e Informática Industrial (RIAI), 3-4, 26-45.

[23] SHINSKEY, F. (1978). *Energy conservation through control.* Academic Press.

[24] SMITH, R. (2005). *Chemical process design and integration.* Wiley.

[25] STODOLA, A. (1945). *Steam and gas turbines.* Vol. 1, Peter Smith, New York.